Sustainable Chemistry and Pharmacy 52 (2026) 102501

Contents lists available at ScienceDirect

Sustainable Chemistry and Pharmacy

journal homepage: www.elsevier.com/locate/scp

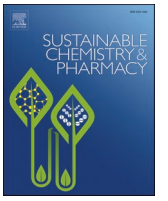

Comparative evaluation of short- and extended-duration ground desert sand powders as mineral additions in cement paste

Mengdi Liu [a], Engui Liu [b,*], Jian Li Hao [b], Luigi Di Sarno [c], Jun Xia [b], Yongchao Zhu [d]

[a] School of Management Science and Engineering, Shandong Technology and Business University, Yantai, Shandong, 264005, China
[b] Department of Civil Engineering, Xi'an Jiaotong-Liverpool University, Suzhou, Jiangsu, 215123, China
[c] Department of Civil and Environmental Engineering, University of Liverpool, L693GH, United Kingdom
[d] College of Railway Engineering, Zhengzhou Railway Vocational & Technical College, Zhengzhou, Henan, 450000, China

ARTICLE INFO

Keywords:
Desert sand powder
Cement paste
Mineral addition
Grinding duration
Strength retention

ABSTRACT

This study compares the cement paste-scale behavior of desert sand powders prepared by short- and extended-duration ball milling under laboratory conditions. The 8 h ground powder, DP1, was compared with a previously reported 12 h ground powder, DP2, used as the extended-duration reference. The powders were characterized by particle size distribution, SEM, XRD, and TGA, and incorporated into cement pastes at 5-20% replacement levels. Semi-adiabatic temperature monitoring, low-field NMR, compressive strength, XRD, TGA, and SEM were used to compare early-age hydration indicators, relative water-state evolution, strength retention, and microstructural features.

Compared with DP1, DP2 showed an earlier temperature response and higher early-age paste strength. This difference decreased with curing age, and DP1-10 and DP2-10 reached similar strengths at 112 days. Desert sand powder reduced strength compared with OPC, particularly at 7, 28, and 56 days. Therefore, the strength results should be interpreted as paste-scale strength retention under cement replacement, rather than strength improvement over OPC. Extended grinding also led to a larger apparent particle size by laser diffraction, attributed to possible secondary agglomeration observed by SEM. Because BET surface area, dispersion-state measurements, agglomerate-breakage tests, and direct reactivity tests were not conducted, the relationship between DP2 particle state and early-age response remains tentative.

Overall, desert sand powder behavior was mainly governed by cement dilution, particle filling, nucleation-related physical effects, water-state evolution, and ongoing cement hydration. Direct chemical contribution or pozzolanic reactivity was not quantified. The results do not establish a universal optimal grinding duration, mortar/concrete-scale performance, or net environmental benefit.

1. Introduction

Cement, as a key component of concrete, has a substantial environmental footprint, contributing an estimated 5%-8% of global anthropogenic CO_2 emissions (Sharp et al., 2010). Reducing cement consumption has therefore become an important strategy to lower the environmental impact of construction materials. Supplementary cementitious materials (SCMs), such as fly ash and ground

* Corresponding author.
E-mail address: engui.liu@xjtlu.edu.cn (E. Liu).

https://doi.org/10.1016/j.scp.2026.102501
Received 18 May 2025; Received in revised form 30 June 2026; Accepted 5 July 2026
Available online 9 July 2026

granulated blast-furnace slag, are widely used to replace cement (Etcheverry et al., 2023) partially. Their incorporation can reduce the environmental impact of cement systems while helping maintain acceptable performance through a combination of physical and chemical effects (Tiwari et al., 2022). In recent decades, the use of conventional SCMs has been challenged by increasing costs, declining availability, and difficulties in ensuring sufficient long-term supply (Xu et al., 2020; Yao et al., 2020a). This has encouraged the exploration of additional local mineral materials for partial cement replacement or as mineral additions in cement-based systems (Suraneni et al., 2019; Zhang et al., 2022).

Desert sand (DS) is an abundant natural material composed mainly of silica-rich minerals, with minor phases such as calcite and clay-related minerals depending on its source (Mohamed and El Gamal, 2009; Gopal, 2006). It is widely distributed across arid and semi-arid regions (Alhozaimy et al., 2012), covering, on average, more than one-tenth of the land area between 30° N and 30° S latitudes (Danin, 1991). Previous studies have mainly investigated desert sand as a fine aggregate in mortar and concrete, where it can partially replace natural river sand and reduce dependence on conventional aggregate resources (Che et al., 2019; Liu et al., 2020; Zhang et al., 2020a; Sajedi, 2012; Wang et al., 2019). These studies have shown that satisfactory mechanical performance can be achieved at suitable replacement levels. Compared with its use as aggregate, however, finely ground desert sand powder as a cement mineral addition has received less attention.

Because desert sand powder is generally quartz-rich, it should not be assumed to behave as a highly reactive pozzolanic SCM. Mechanical grinding can reduce particle size, alter morphology, and modify the surface condition of mineral particles, thereby influencing their interaction with cement paste (Sajedi, 2012; Wang et al., 2019; Wei et al., 2017). For weakly reactive or nominally inert mineral powders, the contribution to cement paste is often associated with physical effects, including cement dilution, particle filling, particle packing, heterogeneous nucleation, and changes in water distribution (Szabó et al., 2023; Guettala and Mezghiche, 2011). For example, previous studies on dune sand powder, quartz powder, and other ground mineral powders have reported that fine particles can influence early-age and hardened properties through filler and nucleation-related effects (Guettala and Mezghiche, 2011; Wu et al., 2017; Lin et al., 2018; Yan and Zhang, 2006). These effects depend strongly on particle size, particle morphology, dispersion state, and cement replacement level.

Grinding duration is an important processing variable for preparing desert sand powder. Longer grinding can further modify powder fineness and morphology, but its effect is not necessarily monotonic. Prolonged milling may promote secondary agglomeration, in which fine particles adhere to one another and form larger clusters (Zhao et al., 2020; Fediuk, 2016). As a result, the apparent particle size measured by laser diffraction may increase even when the primary particles have been further refined. Some studies have reported surface-area-dependent behavior of very fine quartz-containing powders under specific conditions (Benezet and Benhassaine, 1999). Still, direct evidence is required before such behavior can be attributed to intrinsic chemical or pozzolanic reactivity. Therefore, the influence of grinding duration should be evaluated cautiously, particularly when only a limited number of grinding conditions are compared.

Our previous study investigated a 12 h ground desert sand powder as a single cement replacement material (Liu et al., 2023). In the present work, the previously reported 12 h ground powder is designated as DP2 and used as the extended-duration grinding reference. A newly prepared 8 h ground desert sand powder, designated as DP1, is introduced as the short-duration grinding comparison. Selected ordinary Portland cement (OPC) and DP2 datasets from the previous study are included, replotted, reanalyzed, or newly repeated where necessary to provide a consistent reference for comparison with the newly obtained DP1 results.

The objective of this study is to compare the cement paste-scale behavior of short- and extended-duration ground desert sand powders under the present laboratory milling conditions. The comparison focuses on powder characteristics, early-age hydration indicators, relative water-state evolution, compressive strength retention, and representative microstructural features. This study does not aim to establish a universal optimal grinding duration, quantify intrinsic pozzolanic reactivity, or demonstrate mortar/concrete-scale engineering performance. Instead, it examines whether the short-duration powder can maintain comparable paste-scale behavior relative to the extended-duration reference. Further studies on mortar/concrete performance, durability, grinding energy, and life-cycle impact are needed before practical application and environmental benefit can be confirmed.

2. Materials and methods

2.1. Raw materials

The raw materials used in this work included ordinary Portland cement, desert sand, and deionized water. Desert sand was

Fig. 1. Image of cement powder and desert sand powders.

processed in a ball mill for 8 h or 12 h, designated DP1 and DP2, respectively, as shown in Fig. 1. DP2 corresponds to the 12 h ground desert sand powder investigated in our previous study (Liu et al., 2023), where it was evaluated as a single cement replacement material. In the present study, DP2 was used as the extended-grinding reference for comparison with the shorter-duration powder, DP1. The same OPC reference was used to maintain direct comparability between the previously reported DP2 baseline and the newly examined DP1 mixtures. Zirconia balls with diameters of 15 mm, 12 mm, 10 mm, 8 mm, and 5 mm were used as the grinding medium. The desert sand-to-grinding medium ratio was kept at 1:3, and the rotation speed was 300 rpm. Each grinding cycle consisted of 30 min clockwise rotation, 10 min rest, and 30 min counterclockwise rotation, repeated until the target duration was reached.

2.2. Preparation of blended cement mixtures

The desert sand powder was introduced as a cement replacement at 0, 5%, 10%, and 20% by mass, with mix proportions shown in Table 2. The specimens were named in the format of "DP1/DP2-x", where "DP1″ and "DP2″ denote the two desert sand powders described in Section 2.1, and "x" represents the replacement level of desert sand powder in the blended binder. For instance, "DP1-10″ refers to the mixture containing 90% Portland cement and 10% DP1 by mass of binder. To obtain uniform mixtures, cement and desert sand powder were dry mixed for 30 s, followed by an additional 150 s of mixing after water was added. A constant water-to-binder ratio of 0.45 was used for all mixtures to compare paste-scale behavior under a fixed total powder content. Because cement was partially replaced by desert sand powder, the effective water-to-cement ratio increased with increasing replacement level. Therefore, the observed hydration indicators and strength results should be interpreted as the combined outcome of cement dilution, particle filling, particle packing, nucleation-related physical effects, water distribution, and continued hydration of the remaining cement. This mixture design was intended for comparative paste-scale assessment and does not independently distinguish these individual effects or quantify the intrinsic chemical or pozzolanic reactivity of desert sand powder.

The fresh cement paste was cast into 25 mm cube molds and compacted manually. The use of relatively small cube molds for cement paste specimens without sand has been reported in previous studies (Du et al., 2023; Yao et al., 2020b). In this study, as in our previous work on cement paste, 25 mm cube molds were used for all mixtures to ensure direct comparison among pastes prepared under identical conditions. All specimens were demolded after 24 h and cured at 95% relative humidity and 20 ± 2 °C. The cube results are intended for internal comparison among cement paste mixtures only and should not be considered directly equivalent to standard mortar or concrete strength tests.

2.3. Characterization of desert sand and desert sand powder

The particle size distributions of cement and desert sand powder were determined using a laser scattering technique (OMEC LS909). Measurements used alcohol as the dispersion medium for OPC and water for desert sand powder. The measured particle size distributions are reported as apparent particle size distributions under the selected dispersion conditions; therefore, they may reflect both primary particle size and the presence of secondary agglomerates. BET specific surface area, dispersion-state measurements, and agglomerate-breakage tests were not conducted in this study. Desert sand powder morphology was examined using a scanning electron microscope (JEOL, JSM-6510 Series). The powder was mounted on a specimen stub and coated with a thin layer of gold. Secondary electron images were taken at an acceleration voltage of 15 kV. The mineral information of desert sand and desert sand powder was obtained using a Bruker D8 X-ray diffractometer with CuKα radiation. The 2θ range was 5^{o} to 70^{o}, with a step size of 0.01^{o} and a counting time of 0.5 s per step. Jade software was used to analyze the XRD data and match the patterns with the ICDD database. For TGA analysis using a Netzsch STA 449 F^3 analyzer, 250 mg of desert sand or 100 mg of desert sand powder was placed in an alumina crucible and loaded into the furnace. The temperature was raised from 30 °C to 1000 °C at 10 °C/min under a nitrogen atmosphere.

2.4. Hydration heat of blended cement via temperature monitoring

The heat produced by cement paste as it hydrated was measured with a semi-adiabatic calorimetric setup. The setup involved

Table 1
Chemical compositions of cement and desert sand powder (DP).

Chemical compositions	Cement (wt%)	DP (wt%)
Silicon dioxide, SiO_2	18.26	80.74
Aluminum oxide, Al_2O_3	5.24	2.72
Ferric oxide, Fe_2O_3	3.12	0.62
Calcium oxide, CaO	58.27	13.40
Magnesium oxide, MgO	3.10	0.86
Potassium oxide, K_2O	0.68	0.84
Sodium oxide, Na_2O	-	0.52
Sulfur trioxide, SO_3	2.80	0.06
Chlorine, Cl	0.06	0.04

Note: the chemical compositions of cement and desert sand powder were previously reported in Ref (Liu et al., 2023). and are included here to define the material basis for the DP1-DP2 comparison (see Table 1).

Table 2
Proportions of blended cement mixtures by mass ratio of total binder.

Ingredients	OPC	DP1/DP2-5	DP1/DP2-10	DP1/DP2-20
Water	0.45	0.45	0.45	0.45
Cement	1	0.95	0.90	0.80
Desert sand powder	0	0.05	0.10	0.20

keeping the cement paste in an insulated cell with a temperature sensor to track the temperature changes. Around 30 g of powder for each mix was prepared, then dry-mixed in a cup to achieve a uniform mixture. Water was added and manually stirred for 1 min. The mixture was then quickly poured into the specified cell in the polystyrene foam and sealed. The temperature of each specimen was recorded every minute for 48 h, and the first 40 h were used for comparison and presentation in this study. The ambient environment was maintained at about 23 °C and 60% relative humidity. The temperature monitoring method was used to compare early-age hydration behavior among mixtures. It was not used as a direct measurement of fresh properties such as flowability, rheological response, or setting time.

2.5. Blended cement hydration via low-field nuclear magnetic resonance (Low-field NMR)

The water state in the hydrating cement paste was monitored using low-field nuclear magnetic resonance (low-field NMR; Niumag NM21-040H). Approximately 15 g of cement paste was placed into a 25 mm-diameter glass tube for analysis. Testing began approximately 5 min after cement came into contact with water and continued for 72 h, with data collected at 5 min intervals.

The transverse relaxation time (T_2) was recorded to compare the relative evolution of NMR-detectable water during early hydration. For porous materials, the relationship between T_2 and pore geometry is commonly expressed using Eq. (1) (Zhang et al., 2020b; Wang et al., 2017), where T_2 denotes the relaxation time of water in pores, T_{2S} represents the surface relaxation time, ρ_2 is the surface relaxivity, S/V is the surface-to-volume ratio, r is the pore radius, and α is the geometric shape factor, with values of 1, 2, and 3 for planar, cylindrical, and spherical pores, respectively.

$$\frac{1}{T_2} \approx \frac{1}{T_{2S}} = \rho_2 \frac{S}{V} = \rho_2 \frac{\alpha}{r} \quad \text{Eq. 1}$$

In this study, low-field NMR was used only to monitor relative changes in water-state evolution and pore-water confinement during early hydration. Because the surface relaxivity was not independently calibrated, the T_2 results were not converted into absolute pore-size distributions and were not used to quantify hydration-product content or the degree of hydration. The NMR results are therefore interpreted comparatively among mixtures prepared and tested under the same conditions.

2.6. Compressive strength

Hardened cement paste specimens were tested at curing ages of 1, 7, 28, 56, and 112 days. Four specimens from each mixture group were tested to obtain an average. After the compressive strength test, selected specimen portions were crushed into 1-2 cm pieces and soaked in isopropanol for 2 days to stop hydration. These specimens were then dried in a vacuum chamber at room temperature for a day to eliminate isopropanol, readying them for further analysis.

2.7. X-ray diffraction (XRD)

As described in Section 2.6, after the compressive strength tests, selected specimens were collected, hydration was stopped, and the samples were dried. For XRD testing, pieces from these dried specimens were ground to a fine powder, placed in a sample holder, and compacted using a glass slide. The samples were then analyzed using the Bruker D8 X-ray diffractometer, scanning from 5^o to 70^o (2θ) with a step size of 0.01^o and a counting time of 0.5 s per step. All powder samples were loaded into the sample holder with a consistent mass and prepared using the same procedure. Phase identification was performed using Jade software and verified against the ICDD database. XRD was used for phase identification and comparative peak observation. Full quantitative phase analysis by Rietveld refinement was not conducted; therefore, the XRD results cannot be used as direct quantitative proof of the DP reaction degree.

2.8. Thermogravimetric analysis (TGA)

For TGA analysis, the powder samples were prepared using the same procedure as for the XRD samples. Using the Netzsch STA 449 F^3 analyzer, approximately 100 mg of each powder sample was placed in an alumina crucible and heated in the furnace from 30 °C to 1000 °C at 10 °C/min under a nitrogen atmosphere. This process measured weight loss due to phase decomposition, helping identify hydration products and phases such as portlandite and calcite. TGA was used to compare thermal decomposition regions associated with hydration products, portlandite, and carbonate phases. Because DP itself contains carbonate phases and carbonation may also occur during sample handling, the TGA results are interpreted as comparative indicators rather than direct quantitative evidence of chemical or pozzolanic reaction.

2.9. Microstructural morphology

Scanning electron microscopy (SEM) was employed to examine the microstructure of hydration-stopped cement paste specimens. Fragments of hardened cement paste, approximately 1-2 cm in size, were collected after hydration termination. These fragments were mounted on SEM stubs using conductive adhesive and coated with a thin layer of gold for 240 s using an ion sputter coater to enhance conductivity. Imaging was conducted using a JEOL JSM-6510 SEM operating under high-vacuum conditions in secondary-electron mode. All observations were performed immediately following sample preparation to minimize environmental exposure and preserve surface features. SEM observations were used to support a representative microstructural interpretation. They were not used for statistical quantification of pore structure or particle distribution.

This manuscript extends our previous investigation of 12 h ground desert sand powder in blended cement (Liu et al., 2023). In the present manuscript, the 12 h ground powder is denoted as DP2. Selected OPC and DP2 data are reused, replotted, reanalyzed, or newly repeated only to provide a consistent reference for the newly generated DP1 data and the grinding-duration comparison. For each figure, the caption specifies whether the OPC/DP2 data were newly obtained or previously reported. The newly presented contributions include DP1 powder characterization, DP1 blended cement results, DP1-DP2 comparative interpretation, low-field NMR analysis, blended DP1-DP2 powder mixtures, and a revised comparative discussion of paste-scale behavior and methodological limitations.

3. Results and discussion

3.1. Properties of desert sand powder

Fig. 2 shows the particle size distributions of OPC and the two desert sand powders. DP1 and DP2 were both finer than OPC. DP1 had a D50 of 7.4 μm, while DP2 had a larger apparent D50 of 14.3 μm. Because DP2 was produced by longer grinding, this larger apparent size should not be interpreted as coarser primary particles. Instead, it indicated secondary agglomeration during extended milling (Guzzo et al., 2015, 2020), in which fine particles adhered to one another to form larger clusters (Opoczky, 1977). Therefore, the laser diffraction results reflected both the primary particle size and the agglomeration state.

Fig. 3 shows the morphology of OPC, DP1, and DP2, with attention to the aggregation tendency of DP2. Compared with DP1, DP2 showed more rounded particle features and more pronounced particle clustering, indicating that extended grinding modified particle morphology while also promoting secondary agglomeration. This explained why DP2 exhibited a larger apparent particle size in laser diffraction, despite longer grinding. The measured particle size of DP2 therefore reflected both primary particle refinement and agglomerate formation. Similar effects have been reported for finely ground mineral powders, where prolonged milling can alter particle surfaces and increase interparticle interactions, leading to agglomeration (Zhao et al., 2020; Guzzo et al., 2020). The observed aggregation may influence the apparent particle size and early-age hydration response of DP2; however, further BET surface area and dispersion-state measurements would be needed to quantify these effects.

Fig. 4 shows the XRD patterns of the original desert sand (DS), DP1, and DP2. Quartz and calcite were identified as the main crystalline phases, with minor clay-related peaks observed in the original desert sand. After grinding, the clay-related peaks became less visible or were no longer clearly detected, which may reflect reduced crystallinity, preferential grinding of softer clay minerals, or a decrease in peak intensity below the detection limit of XRD (Souri et al., 2015; Cheng et al., 2021). The calcite peak around 29.5° also became broader after grinding, particularly for DP2, suggesting grinding-induced structural disorder, reduced crystallite size, or partial modification of the calcite-containing phase (Kumar et al., 2008). In contrast, the quartz peaks remained clearly detectable in

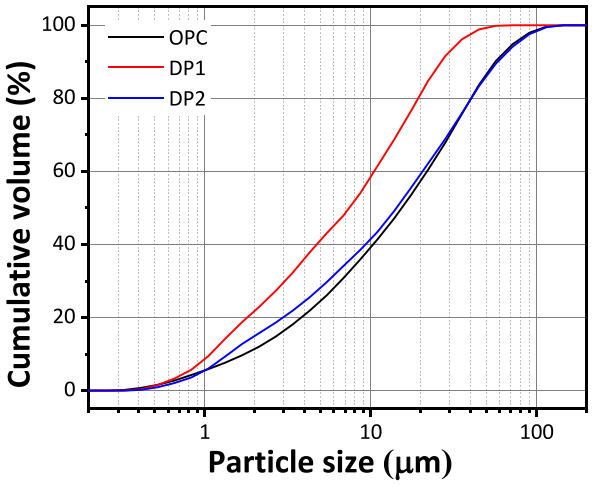

Fig. 2. Particle size distributions of OPC and desert sand powders. OPC and DP2 correspond to the previously reported reference cement and 12 h ground desert sand powder (Liu et al., 2023), while DP1 was introduced in the present study as the short-duration grinding comparison.

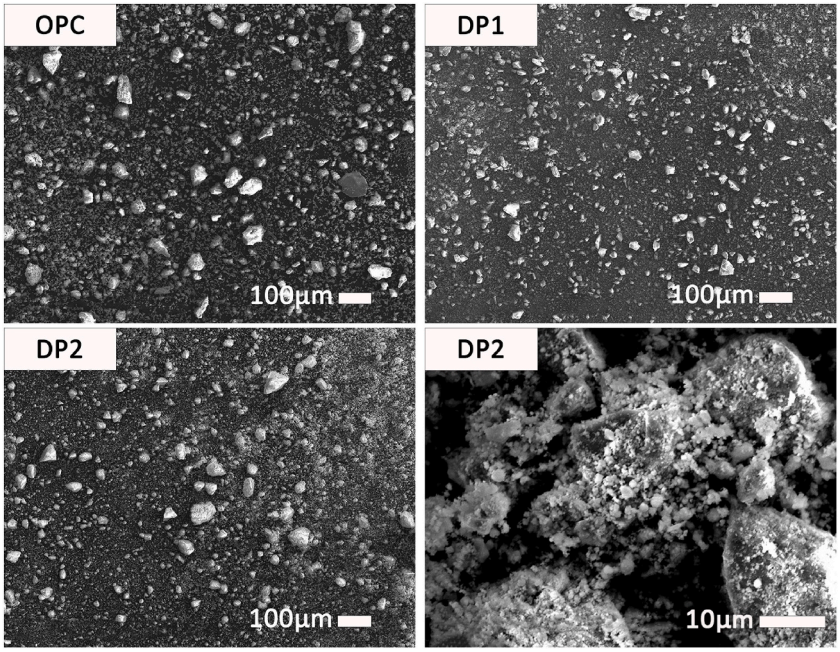

Fig. 3. Surface morphology of OPC and desert sand powders. Although OPC and DP2 were previously investigated, all images shown here were newly acquired for the present DP1-DP2 comparison. The bottom-right image highlights particle aggregation in DP2.

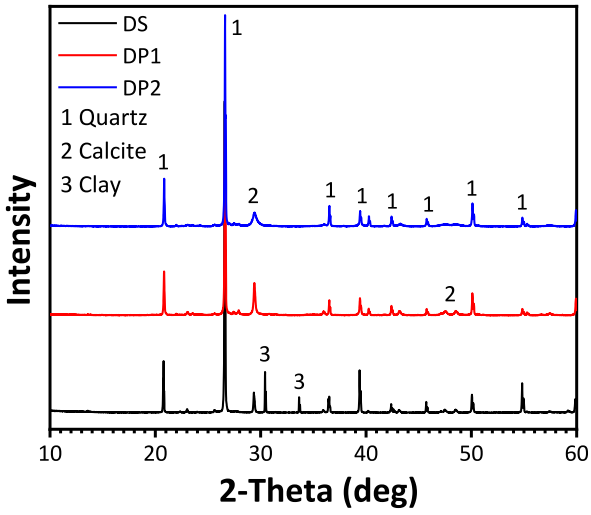

Fig. 4. XRD patterns of original desert sand and desert sand powders. DP2 corresponds to the previously reported 12 h ground powder (Liu et al., 2023) and is included as the extended-grinding reference for comparison with DP1.

both DP1 and DP2, indicating that quartz remained the dominant crystalline phase after grinding. The XRD results supported grinding-induced physical and structural modification of desert sand powder, but they did not provide quantitative evidence of chemical or pozzolanic reactivity.

Fig. 5 shows the TGA/DTG curves of desert sand, DP1, and DP2. Mass loss below approximately 150 °C was mainly associated with adsorbed water, while the region around 400 °C may include clay-related dehydroxylation and possible portlandite decomposition. The main mass loss between 600 °C and 900 °C corresponded mainly to carbonate decomposition. DP2 showed higher low-temperature mass loss than DP1, suggesting stronger moisture adsorption or a higher amount of surface-associated water after extended grinding. The lower-temperature shoulder in the carbonate decomposition region indicated that grinding may have modified the carbonate phase. However, these changes should be interpreted as evidence of grinding-induced structural modification (Li et al., 2014), not as direct proof of changes in chemical properties or reactivity in blended cement.

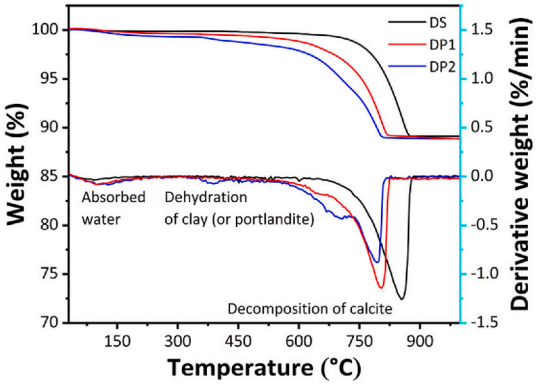

Fig. 5. TGA/DTG curves and associated mass-loss regions of desert sand and desert sand powders. DP2 corresponds to the previously reported 12 h ground powder (Liu et al., 2023) and is included as the extended-grinding reference.

3.2. Hydration heat of blended cement via temperature measurement

Figs. 6 and 7 show the temperature evolution of cement pastes containing DP1 or DP2 over 40 h. The temperature curves were used as comparative indicators of early-age hydration behavior. The heat-release process followed the typical stages of initial reaction, induction, acceleration, and deceleration (Thongsanitgarn et al., 2014). The incorporation of desert sand powder changed the initial temperature response compared with OPC, which may be associated with cement dilution, additional particle surfaces for heterogeneous nucleation, changes in particle packing, and differences in water distribution (Panesar and Zhang, 2020; Mehdizadeh et al., 2020; Knop and Peled, 2016). These effects may also be related to early structural build-up in the paste. However, direct fresh-property measurements such as flow, rheology, and setting time were not conducted in this study.

Mixtures containing DP2 showed an earlier initial temperature response than those containing DP1. This indicates that the extended-duration ground powder produced a stronger apparent early-age temperature response under the present test conditions. However, because BET surface area, dispersion state, agglomerate-breakage behavior, dissolution behavior, and cement-mass-normalized calorimetry were not measured, this result should not be interpreted as direct evidence of higher intrinsic chemical or pozzolanic reactivity. Instead, the different response of DP2 is more cautiously attributed to the combined influence of particle morphology, apparent particle state, packing, nucleation-related physical effects, cement dilution, and water distribution.

DP1 mixtures exhibited a delayed primary temperature peak compared with OPC, particularly at higher replacement levels. This delay was mainly attributed to cement dilution and to the increased effective water-to-cement ratio resulting from cement replacement (Thongsanitgarn et al., 2014). In contrast, DP2 mixtures showed primary reaction times closer to OPC. This suggests that DP2 affected the early-age temperature evolution more strongly than DP1, but the mechanism should be understood primarily as an apparent paste-scale response rather than as confirmed chemical reactivity of desert sand powder.

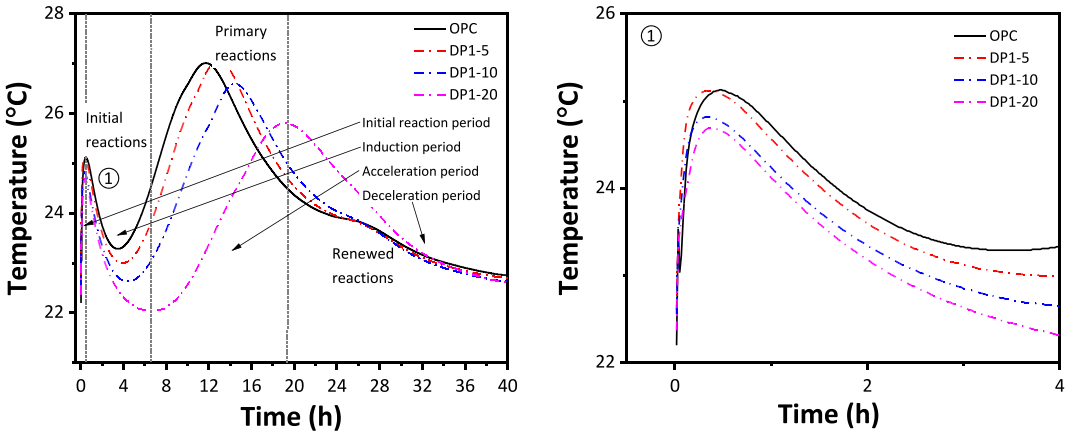

Fig. 6. Hydration temperature evolution of OPC and DP1 blended cement mixtures. The OPC reference is included to provide a consistent baseline for comparison; DP1 mixtures were newly evaluated in this study. The right column shows an enlarged view of the section highlighted in the left column, indicated by ①

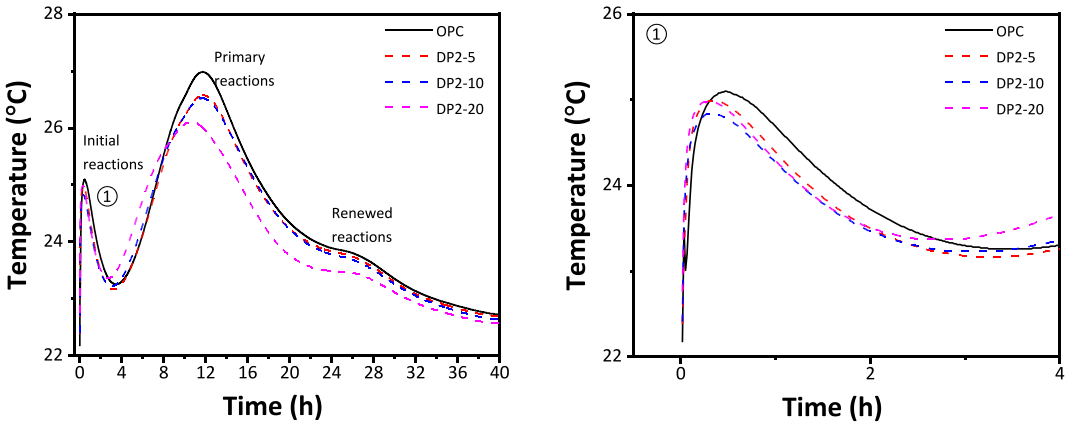

Fig. 7. Hydration temperature evolution of OPC and DP2 blended cement mixtures. DP2 corresponds to the 12 h ground desert sand powder previously investigated in Ref. (Liu et al., 2023). The temperature curves shown here were obtained from an independent, repeated experiment conducted for the present DP1-DP2 comparison and serve as the extended-grinding reference. The right column shows an enlarged view of the section highlighted in the left column, indicated by ①

3.3. Low-field NMR of blended cement hydration

Fig. 8 shows the change of T_2 relaxation-time distributions over time for OPC, DP1-10, and DP2-10 cement pastes. In this study, low-field NMR was used to compare the relative evolution of NMR-detectable water during early hydration. Because the surface relaxivity was not independently calibrated, the T_2 results were not converted into absolute pore-size distributions and were not used to quantify hydration-product content or degree of hydration. Therefore, the NMR results are interpreted only as relative indicators of water-state evolution among mixtures prepared and tested under the same conditions.

Shorter T_2 values generally correspond to stronger water confinement, while longer T_2 values indicate relatively less confined water (She et al., 2021; Jiang et al., 2022). As hydration proceeded, the T_2 distributions of all mixtures shifted toward shorter relaxation times, which is consistent with progressive water consumption and increasing confinement of pore water during cement hydration. During the early period, two relaxation regions could be observed: a longer-relaxation region associated with less confined water and a shorter-relaxation region associated with more confined water. These regions are used here for comparative interpretation only and should not be treated as quantitatively calibrated pore classes.

The weighted mean T_2 values in Fig. 9 (left) provide a comparative indication of water-state evolution during early hydration. At the initial stage, the DP-containing mixtures showed higher T_2 values than OPC, which may be related to cement dilution and increased effective water availability. DP1-10 showed a slightly shorter relaxation time than DP2-10 at early age, possibly due to its finer apparent particle size and different packing behavior. With hydration, all mixtures showed decreasing weighted mean T_2 values, indicating increased water confinement under the same testing conditions.

The integrated T_2 peak area in Fig. 9 (right) reflects changes in the NMR-detectable water signal during hydration (She et al., 2021). After approximately 400 min, the decrease in peak area was consistent with continued water consumption and redistribution during hydration. DP2-10 showed a faster decrease in peak area during the acceleration period, which agreed with the temperature-monitoring results. However, this observation should be interpreted as a relative water-state response and not as quantitative evidence of higher hydration degree or improved pore structure.

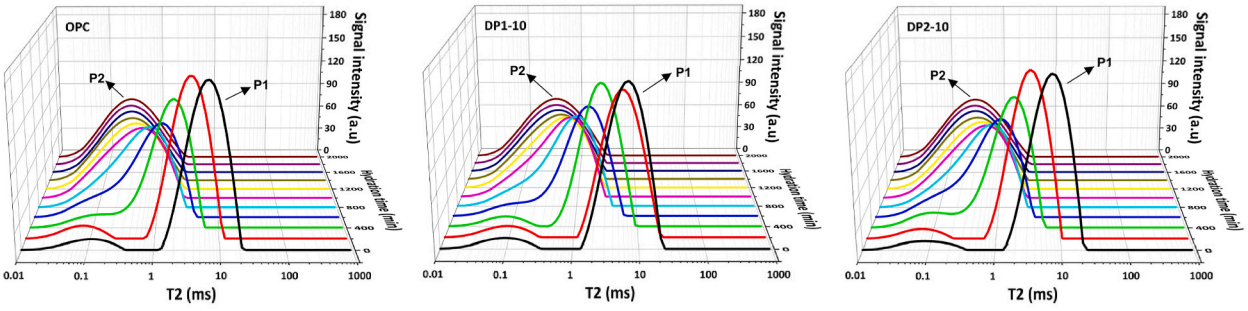

Fig. 8. Low-field NMR T_2 distributions of hydrating OPC, DP1-10, and DP2-10 cement pastes. These measurements were used to compare water-state evolution during early hydration.

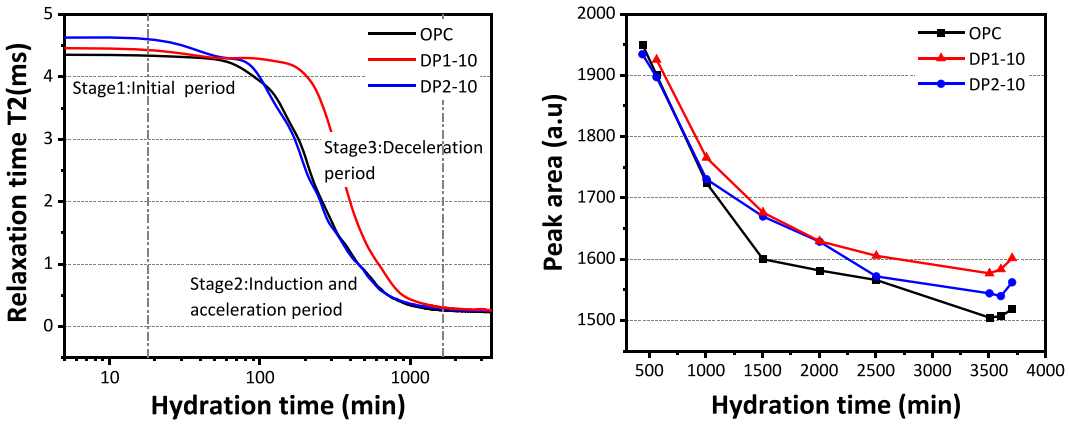

Fig. 9. Temporal evolution of the weighted mean relaxation time (T_2) (Left) and integrated peak area (Right) of hydrating cement mixtures, assessing water-state evolution among OPC, DP1-10, and DP2-10 mixtures.

3.4. Compressive strength

Fig. 10 (left) shows the compressive strength of OPC and blended cement pastes during the 112-day curing period. The incorporation of desert sand powder generally reduced compressive strength compared with OPC, especially at 7, 28, and 56 days. This reduction was expected because partial cement replacement decreased the amount of clinker available for hydration and increased the effective water-to-cement ratio when the water-to-binder ratio was kept constant. Therefore, the strength results should be interpreted mainly in terms of strength retention under cement replacement, rather than as strength improvement over OPC.

Despite the dilution effect, the strength difference between OPC and the low-replacement DP mixtures became smaller at later curing ages. At 112 days, the 5% and 10% DP mixtures reached strengths close to the OPC reference. As shown by the strength-growth rate in Fig. 10 (right), the strength gain of OPC became limited after 56 days, whereas several DP-containing mixtures continued to show measurable strength development from 56 to 112 days. This late-age strength gain may be associated with continued hydration of the remaining cement, particle filling, nucleation-related physical effects, gradual densification of the paste matrix, and the lower dilution effect at moderate replacement levels. It should not be taken as direct evidence of intrinsic chemical or pozzolanic reactivity of desert sand powder.

Comparing the two grinding durations, DP2 showed higher early-age strength than DP1. For example, at 7 days, DP2-10 reached about 46 MPa, while DP1-10 reached about 26 MPa. This agreed with the temperature-monitoring and low-field NMR results, which indicated a stronger apparent early-age response for DP2. However, this difference decreased with curing time. At 112 days, DP1-10 and DP2-10 reached similar strengths, suggesting that long-term paste strength became less sensitive to the difference between the two grinding durations under the present conditions. Therefore, extended-duration grinding appeared mainly to shift part of the strength development to earlier ages, while the shorter-duration powder showed slower but more sustained strength gain. This interpretation is limited to the desert sand source, milling equipment, replacement levels, and cement paste system used in this study.

To further compare strength retention after cement replacement, the strength activity index (SAI) was calculated as the compressive strength ratio between each DP-blended cement paste and the OPC reference at the same curing age. The SAI was used as a comparative strength-retention indicator rather than as direct proof of reactivity or formal qualification as an SCM. The results showed

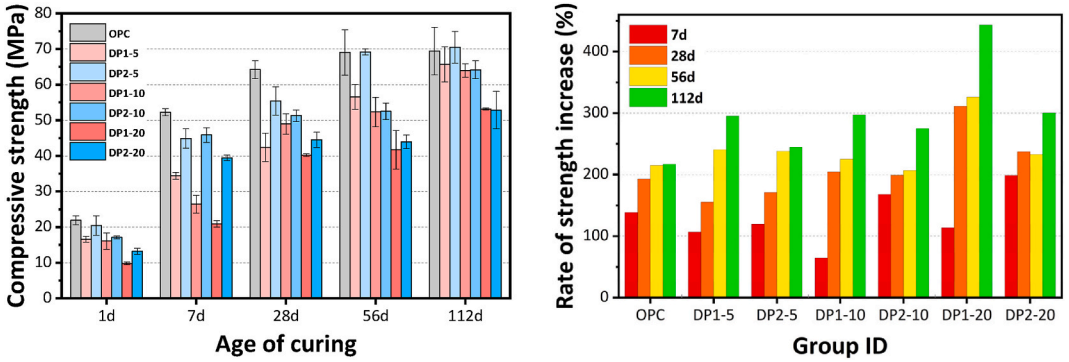

Fig. 10. Compressive strength (Left) and strength growth rate (Right) of OPC, DP1, and DP2 blended cement pastes. OPC and DP2 datasets that were previously reported for the 12 h ground desert sand powder system (Liu et al., 2023) are replotted here as reference data; DP1 datasets were newly obtained for the grinding-duration comparison.

that moderate DP replacement retained a substantial proportion of the OPC strength, especially at later curing ages. Among the replacement levels directly tested, 10% DP produced lower strength loss than 20% replacement while allowing greater cement reduction than 5% replacement. Therefore, 10% DP can be considered a reasonable paste-scale replacement level within the tested range, rather than a universal optimum. The 20% replacement level showed a stronger dilution effect and would require further mixture optimization before practical use.

3.5. X-ray diffraction analysis

Fig. 11 shows the XRD patterns of hydrated OPC, DP1-10, and DP2-10 pastes at 1, 28, and 112 days. The main phases identified included residual clinker phases, ettringite, portlandite, calcite, quartz, and carbonate-containing AFm phases. In blended cement pastes, quartz mainly originated from desert sand powder, while calcite could originate from both desert sand powder and carbonation. Carbonate-AFm formation was consistent with the interaction between carbonate phases and aluminate-bearing cement hydration products.

Compared with DP1-10, DP2-10 showed greater early-age changes in the relative intensities of clinker-related and hydration-product peaks. This observation was consistent with the hydration-temperature and NMR results, suggesting a stronger apparent

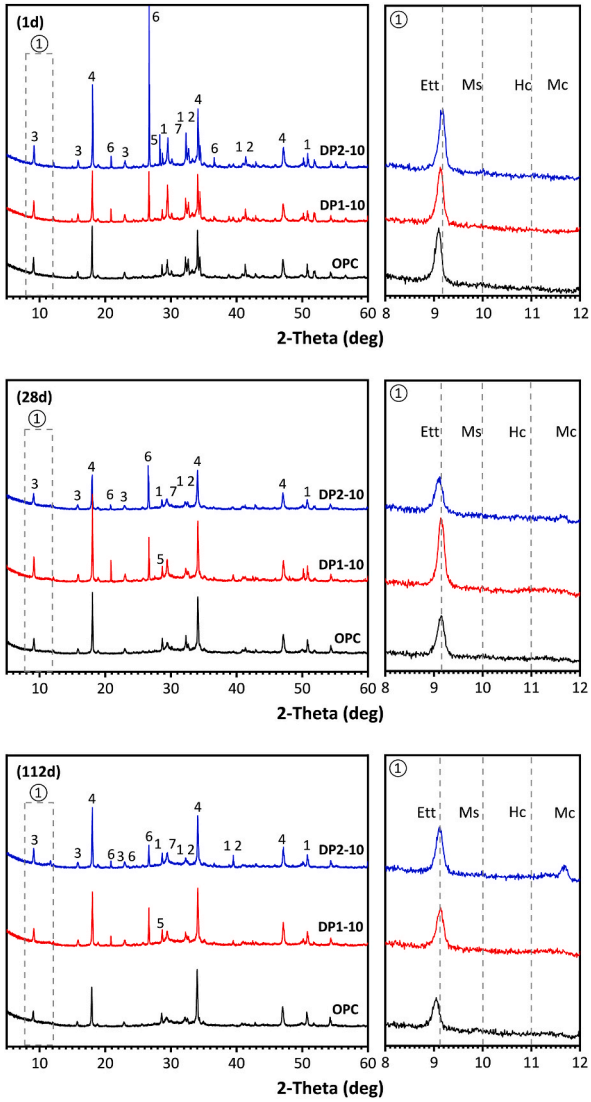

Fig. 11. XRD patterns of hydrated cement paste at curing ages of 1, 28, and 112 days, displaying the main phases: 1 - Calcium Silicates (C_3S); 2 - Larnite (C_2S); 3 - Ettringite; 4 - Portlandite; 5 - C-S-H (II); 6 - Quartz; 7 - Calcite. Additional notations include Ett (Ettringite), Ms (Mono-sulfate), Hc (Hemi-carbonate), and Mc (Mono-carbonate); OPC and DP2-10 patterns previously reported for the 12 h ground powder system (Liu et al., 2023) are included as reference data, where applicable.

early-age hydration response for DP2. After 28 days, carbonate-containing AFm phases were more clearly observed in the blended cement pastes, particularly in DP2-10. However, because quantitative phase analysis by Rietveld was not conducted, the XRD results should be interpreted qualitatively. The reduction or variation in the intensities of the portlandite and quartz peaks cannot, by itself, serve as quantitative proof of a chemical or pozzolanic reaction. Therefore, the XRD evidence supported comparative phase evolution but did not independently quantify chemical reaction or pozzolanic reactivity of DP.

3.6. Thermogravimetric analysis

Fig. 12 shows the TGA/DTG curves of OPC, DP1-10, and DP2-10 hydrated cement pastes at 1, 28, and 112 days. The mass loss below approximately 400 °C was mainly associated with the removal of physically bound water and the dehydration of hydration products such as C-S-H, AFt, and AFm (Yao et al., 2020a; Kumar et al., 2008; Jeong et al., 2020). The mass-loss region between approximately 400 °C and 600 °C was commonly associated with portlandite decomposition (Jeong et al., 2020), while the region between approximately 600 °C and 850 °C was mainly related to carbonate decomposition (Kumar et al., 2008). Because the desert sand powder itself contains carbonate phases, and hydrated cement pastes may also undergo carbonation during curing, drying, or storage, the carbonate-related mass loss cannot be uniquely assigned to either original DP calcite or newly formed carbonate-containing hydrates.

DP2-10 showed a larger early-age mass loss in the low-temperature region than DP1-10, indicating a stronger early-age hydration-related thermal response, consistent with the temperature-monitoring and low-field NMR results. With increasing curing age, the difference between DP1-10 and DP2-10 became less pronounced, which agreed with the compressive strength results showing that the

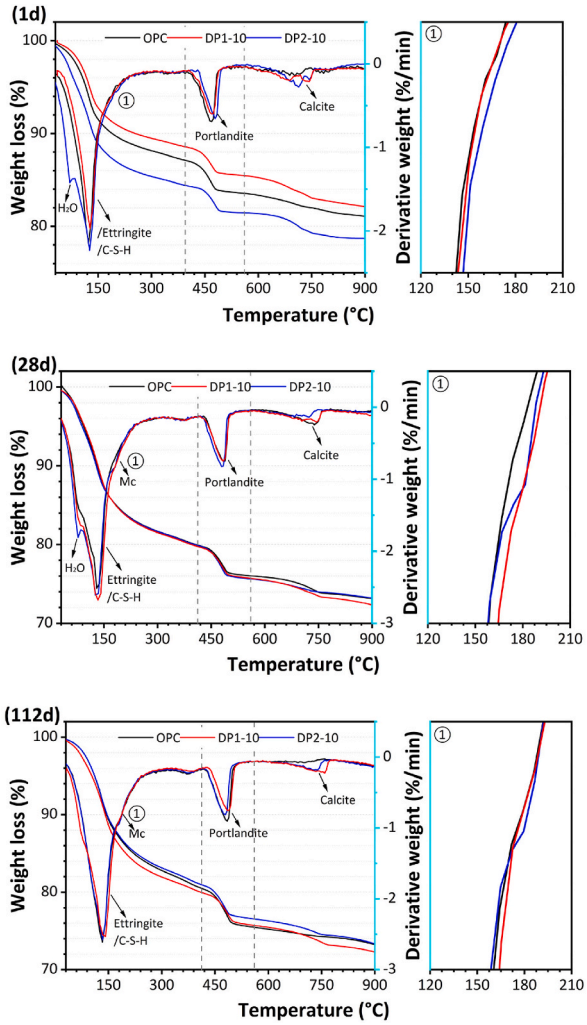

Fig. 12. TGA/DTG curves of hydrated cement paste at 1, 28, and 112 days. The left column shows the full profiles of weight loss and the corresponding derivative weight curves, while the right column presents an enlarged view of the region marked ① in the left column; OPC and DP2-10 patterns previously reported for the 12 h ground powder system (Liu et al., 2023) are included as reference data where applicable.

early-age strength advantage of DP2 decreased at later ages. Therefore, the TGA results support the interpretation that extended-duration grinding mainly affected early-age paste behavior, while its influence on long-term paste strength became less significant.

Fig. 13 summarizes the TGA-derived portlandite-related and carbonate-related indicators. The OPC paste showed a gradual increase in the portlandite-related signal with curing age, reflecting continued cement hydration. In contrast, DP1-10 and DP2-10 showed lower portlandite-related values than OPC, which can be attributed primarily to cement dilution and differences in hydration development. Because portlandite consumption was not normalized by cement content and direct reactivity tests were not conducted, the portlandite-related results should be interpreted as comparative indicators of hydration and phase evolution, rather than as direct evidence of intrinsic DP reactivity.

The carbonate-related signal reflected the combined contribution of carbonate originally present in desert sand powder, carbonate-bearing hydration products, and possible carbonation of hydration phases. The higher carbonate-related values in DP-containing pastes were therefore expected because DP contained calcite. Changes in this signal with curing age may indicate carbonate redistribution, formation of carbonate-bearing AFm phases, or carbonation-related changes, but they cannot be used alone to quantify calcite consumption or chemical reaction of DP. Overall, the TGA results were consistent with the XRD observations and support a cautious interpretation in which desert sand powder contributed mainly through cement dilution, particle filling, nucleation-related physical effects, carbonate-bearing phase evolution, and continued hydration of the remaining cement.

3.7. Micromorphology analysis

Fig. 14 presents SEM images of OPC, DP1-10, and DP2-10 pastes cured for 1 and 28 days. After 1 day, all samples exhibited typical early hydration products, including ettringite, C-S-H, and unreacted cement grains. In the DP-containing pastes, desert sand powder particles were embedded in the hydrated matrix and partially covered by hydration products. At 1 day, DP2-10 showed a more continuous and interconnected microstructure than DP1-10, which exhibited a relatively looser matrix. This observation was consistent with the temperature-monitoring, NMR, and compressive-strength results, which indicated a stronger apparent early-age response for DP2-10.

After 28 days, all samples developed denser microstructures. Compared with DP1-10, DP2-10 exhibited a more compact and homogeneous matrix with fewer visible local gaps. This trend agrees with its higher strength at the same age. Overall, the SEM observations indicate that desert sand powder was incorporated into the hydrated cement matrix and that DP2-10 showed a more continuous representative microstructure than DP1-10. However, SEM observations are qualitative and local. They should not be used as statistical evidence of pore refinement, reaction degree, or intrinsic chemical reactivity.

3.8. Effects of combining two desert sand powders on blended cement properties

Experiments were conducted to examine the effect of combining DP1 and DP2 at 5% replacement each. The resulting DP1-5+DP2-5 mixture was compared with DP1-10 and DP2-10 to determine whether combining powders prepared by different grinding durations changed the paste-scale behavior relative to using each powder individually. As shown in Fig. 15, the compressive strength of DP1-5+DP2-5 was lower than that of either DP1-10 or DP2-10, especially at early and middle curing ages. After 28 days, its strength became closer to that of DP1-10 and DP2-10, although it remained lower. A similar tendency was observed in the TGA results, where the total hydration-related mass loss of DP1-5+DP2-5 was lower than that of DP1-10 and DP2-10 after 28 days.

These results indicate that simply combining powders prepared by different grinding durations did not improve the strength retention or hydration-related thermal response under the present paste conditions. One possible explanation is that the combination of relatively angular DP1 particles and more agglomerated DP2 particles may have increased local clustering, thereby reducing effective dispersion and packing in the paste. This could have influenced local water distribution and delayed part of the hydration process. However, because packing density, dispersion state, and agglomerate-breakage behavior were not directly measured, this explanation should be considered tentative. The result further suggests that the benefit of extended grinding should be evaluated

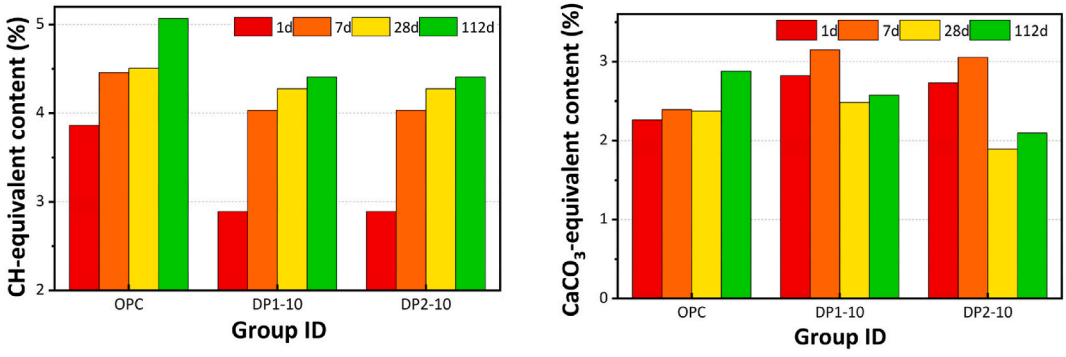

Fig. 13. TGA-derived CH-equivalent (Left) and $CaCO_3$-equivalent (Right) contents for OPC, DP1-10, and DP2-10 cement pastes, calculated from the corresponding decomposition regions and used as comparative phase-evolution indicators.

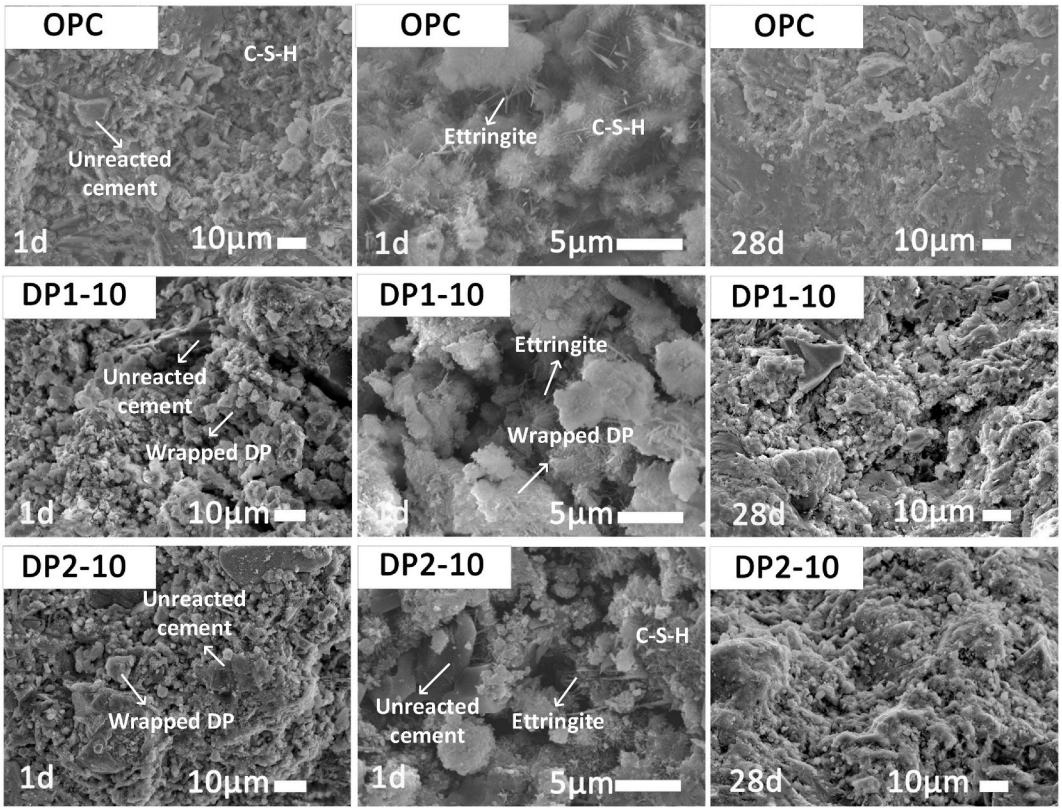

Fig. 14. SEM images of hydrated OPC, DP1-10, and DP2-10 cement pastes. Although OPC and DP2 were previously investigated, all SEM images shown here were newly acquired for the present DP1-DP2 comparison.

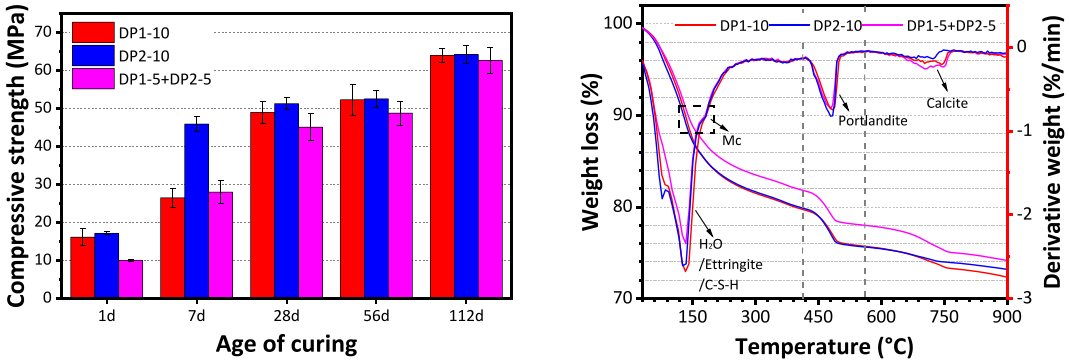

Fig. 15. Comparison of compressive strength (Left) and hydration-related mass loss (Right) of DP1-10, DP2-10, and DP1-5+DP2-5 cement pastes. The DP1-5+DP2-5 mixture was newly designed to evaluate whether combining powders with different grinding durations changes paste-scale behavior.

together with possible agglomeration and processing demand.

3.9. Comparative interpretation and limitations

The results show that the two desert sand powders produced different paste-scale responses under the present laboratory milling conditions. DP2, the extended-duration ground powder, showed an earlier temperature response, faster relative water-state evolution, and higher early-age compressive strength than DP1. However, DP2 also showed a larger apparent particle size in laser diffraction, which was attributed to possible secondary agglomeration. Because BET surface area, dispersion-state measurements, agglomerate-breakage tests, and direct reactivity tests were not conducted, the link between DP2 particle state and its early-age response

remains tentative.

The comparison between DP1 and DP2 suggests that the main difference between the two powders was reflected at early ages. At long curing ages, especially at 112 days, DP1-10 and DP2-10 reached similar compressive strengths. Therefore, within the tested cement paste system, the shorter-duration powder was able to maintain comparable long-term paste strength, while the extended-duration powder mainly showed stronger early-age indicators. This finding should not be interpreted as a universal grinding-duration rule or an optimal grinding duration, because grinding efficiency depends on sand mineralogy, initial particle size, mill type, grinding media, ball-to-powder ratio, powder loading, grinding speed, and dispersion state.

Mechanistically, the role of desert sand powder should be interpreted cautiously. The powder was quartz-rich and should not be assumed to behave as a highly reactive pozzolanic SCM. The observed behavior is more reasonably attributed to the combined effects of cement dilution, particle filling, particle packing, nucleation-related physical effects, carbonate-bearing phase evolution, water-state evolution, and continued hydration of the remaining cement. The XRD and TGA results supported comparative phase evolution, but they did not quantify DP reaction. The NMR results showed relative water-state evolution, but they did not provide calibrated pore-size distribution, hydration-product content, or hydration degree. The SEM observations provided representative microstructural evidence, but they did not provide statistical pore-structure or reaction-degree information.

The strength results should also be understood in terms of strength retention rather than strength enhancement. The DP-containing pastes generally showed lower strength than OPC, especially at 7, 28, and 56 days. The later-age strength of the 5% and 10% replacement mixtures approached the OPC reference mainly because the dilution effect was limited at moderate replacement levels and because continued hydration and physical filling helped maintain paste strength. Therefore, the present results indicate that acceptable paste-scale strength can be maintained at moderate replacement levels, but they do not show that desert sand powder improves strength relative to OPC.

The sustainability implications also require caution. Replacing part of the cement with desert sand powder reduces the cement fraction in the binder. However, the net environmental benefit cannot be confirmed without considering grinding energy, transport distance, processing scale, and local material availability. A full life-cycle assessment was not conducted in this study. Therefore, the present work should be regarded as a paste-scale material assessment rather than proof of environmental advantage. Future studies should quantify grinding energy and transport scenarios for different milling conditions before the net CO_2 benefit of desert sand powder can be evaluated.

Lastly, the present study was limited to cement paste specimens, replacement levels of 0-20%, and two grinding durations selected to represent short- and extended-duration grinding under the present laboratory conditions. The results cannot be directly generalized to mortar or concrete. Future work should examine a broader range of desert sand sources to account for regional variations in quartz, carbonate minerals, clay minerals, and impurities. The research should also be extended to mortar and concrete, including fresh properties such as flow, rheology, and setting time, as well as durability indicators such as drying shrinkage, carbonation, water permeability, chloride penetration, sulfate resistance, and freeze-thaw resistance. These additional tests are necessary before desert sand powder can be evaluated for practical engineering applications.

4. Conclusions

This study compared the cement paste-scale behavior of desert sand powders prepared by short- and extended-duration ball milling under the present laboratory conditions. An 8 h ground powder, designated as DP1, was compared with a previously reported 12 h ground powder, designated as DP2, which was used as the extended-duration reference. The study was limited to the tested desert sand source, milling conditions, replacement levels, and cement paste specimens. Based on the results, the following conclusions can be drawn:

(1) Mechanical grinding modified the particle size distribution, morphology, mineral-phase characteristics, and thermal behavior of desert sand powder. DP1 and DP2 were both finer than OPC. However, the extended-duration ground powder did not show a smaller apparent particle size in laser diffraction. DP2 showed a larger apparent D50 than DP1, which was attributed to possible secondary agglomeration observed in SEM. Because BET surface area, dispersion-state measurements, and agglomerate-breakage tests were not conducted, this interpretation should be regarded as tentative.

(2) DP2 showed an earlier temperature response and faster relative water-state evolution than DP1 at early age. This indicates that the extended-duration ground powder had a stronger apparent early-age response under the present cement paste conditions. However, these results should be interpreted mainly in terms of particle morphology, apparent particle state, particle packing, nucleation-related physical effects, cement dilution, and water distribution. They do not provide direct evidence of intrinsic chemical or pozzolanic reactivity of desert sand powder.

(3) The incorporation of desert sand powder generally reduced compressive strength compared with OPC, especially at 7, 28, and 56 days. Therefore, the strength results should be interpreted as strength retention under cement replacement, rather than strength improvement over OPC. DP2 achieved higher early-age strength than DP1; for example, DP2-10 reached about 46 MPa at 7 days, compared with about 26 MPa for DP1-10. However, this difference decreased with curing age, and DP1-10 and DP2-10 reached similar strengths at 112 days. This suggests that extended-duration grinding mainly affected early-age paste behavior, while long-term strength became less sensitive to the difference between the two grinding durations.

(4) Among the replacement levels directly tested, 10% desert sand powder produced lower strength loss than 20% replacement while allowing greater cement reduction than 5% replacement. Therefore, 10% replacement can be considered a reasonable

paste-scale replacement level within the tested range. It should not be described as a universal optimum. The 20% replacement level showed a stronger dilution effect and would require further mixture optimization.

(5) XRD, TGA, and SEM results supported the comparative interpretation of phase evolution and representative microstructural development in DP-containing cement pastes. However, these methods did not quantify the reaction degree of desert sand powder. The XRD results were qualitative; the TGA-derived portlandite- and carbonate-related indicators could not independently prove chemical reaction, and the SEM images were representative rather than statistical. Therefore, desert sand powder should be regarded in this study as a quartz-rich mineral addition rather than a proven highly reactive supplementary cementitious material.

(6) The present results do not establish a universal optimal grinding duration, mortar/concrete-scale engineering performance, or net environmental benefit. Grinding efficiency and powder behavior depend on sand mineralogy, milling equipment, grinding media, ball-to-powder ratio, powder loading, grinding speed, and dispersion state. Further work is needed to quantify BET surface area, dispersion, agglomeration, intrinsic reactivity, grinding energy, transport-related emissions, fresh properties, durability, and mortar/concrete-scale performance before practical application and life-cycle benefit can be confirmed.

CRediT authorship contribution statement

Mengdi Liu: Investigation, Methodology, Visualization, Writing – original draft. **Engui Liu:** Conceptualization, Supervision, Writing – original draft, Writing – review & editing. **Jian Li Hao:** Supervision, Writing – review & editing. **Luigi Di Sarno:** Supervision, Writing – review & editing. **Jun Xia:** Supervision, Writing – review & editing. **Yongchao Zhu:** Investigation, Writing – review & editing.

Declaration of competing interest

The authors declared that they have no conflicts of interest to this work.

Acknowledgments

This research was supported by the Xi'an Jiaotong-Liverpool University (XJTLU) Research Development Funding (RDF-19-01-22), alongside contributions from the Department of Civil Engineering and the Department of Chemistry and Materials Science at XJTLU. Acknowledgments also go to the Suzhou Industrial Park High Quality Innovation Platform of Functional Molecular Materials and Devices (YZCXPT2023105), the XJTLU Advanced Materials Research Center (AMRC).

Data availability

Data will be made available on request.

References

Alhozaimy, A., Al-Negheimish, A., Alawad, O.A., Jaafar, M.S., Noorzaei, J., 2012. Binary and ternary effects of ground dune sand and blast furnace slag on the compressive strength of mortar. Cem. Concr. Compos. 34, 734–738. https://doi.org/10.1016/j.cemconcomp.2012.03.002.

Benezet, J.C., Benhassaine, A., 1999. The influence of particle size on the pozzolanic reactivity of quartz powder. Powder Technol. 103, 26–29.

Che, J., Wang, D., Liu, H., Zhang, Y., 2019. Mechanical properties of desert sand-based fiber reinforced concrete (DS-FRC). Appl. Sci. 9. https://doi.org/10.3390/app9091857.

Cheng, S., Ge, K., Sun, T., Shui, Z., Chen, X., Lu, J.X., 2021. Pozzolanic activity of mechanochemically and thermally activated coal-series kaolin in cement-based materials. Constr. Build. Mater. 299, 123972. https://doi.org/10.1016/j.conbuildmat.2021.123972.

Danin, A., 1991. Plant adaptations in desert dunes. J. Arid Environ. 21, 193–212. https://doi.org/10.1016/s0140-1963(18)30682-7.

Du, J., Zhang, T., Chen, P., Guo, Y., Zhan, B., Wei, J., Yu, Q., 2023. Phase separation of recycled concrete powder during grinding and consequent influences on its hydration behaviors in cement paste. Cem. Concr. Compos. 142, 105203. https://doi.org/10.1016/j.cemconcomp.2023.105203.

Etcheverry, J.M., Yue, Z., Krishnan, S., Villagran-Zaccardi, Y.A., Van den Heede, P., Dhandapani, Y., Bernal, S.A., De Belie, N., 2023. Phase evolution of hybrid alkali sulfate-activated ground-granulated blast furnace slag cements. ACS Sustain. Chem. Eng. 11, 17519–17531. https://doi.org/10.1021/acssuschemeng.3c05937.

Fediuk, R.S., 2016. Mechanical activation of construction binder materials by various mills. IOP Conf. Ser. Mater. Sci. Eng. 125. https://doi.org/10.1088/1757-899X/125/1/012019.

Gopal, R., 2006. Polymer concrete composites for enhancement of mobility of troops in desert operations. Mater. Sci. Eng. B Solid-State Mater. Adv. Technol. 132, 129–133. https://doi.org/10.1016/j.mseb.2006.04.001.

Guettala, S., Mezghiche, B., 2011. Compressive strength and hydration with age of cement pastes containing dune sand powder. Constr. Build. Mater. 25, 1263–1269. https://doi.org/10.1016/j.conbuildmat.2010.09.026.

Guzzo, P.L., Marinho de Barros, F.B., Soares, B.R., Santos, J.B., 2020. Evaluation of particle size reduction and agglomeration in dry grinding of natural quartz in a planetary ball mill. Powder Technol. 368, 149–159. https://doi.org/10.1016/j.powtec.2020.04.052.

Guzzo, P.L., Tino, A.A.A., Santos, J.B., 2015. The onset of particle agglomeration during the dry ultrafine grinding of limestone in a planetary ball mill. Powder Technol. 284, 122–129. https://doi.org/10.1016/j.powtec.2015.06.050.

Jeong, Y., Kang, S.H., Kim, M.O., Moon, J., 2020. Acceleration of cement hydration from supplementary cementitious materials: performance comparison between silica fume and hydrophobic silica. Cem. Concr. Compos. 112, 103688. https://doi.org/10.1016/j.cemconcomp.2020.103688.

Jiang, D., Li, X., Lv, Y., Li, C., Zhang, T., He, C., Leng, D., Wu, K., 2022. Early-age hydration process and autogenous shrinkage evolution of high performance cement pastes. J. Build. Eng. 45, 103436. https://doi.org/10.1016/j.jobe.2021.103436.

Knop, Y., Peled, A., 2016. Setting behavior of blended cement with limestone: influence of particle size and content. Mater. Struct. Constr. 49, 439–452. https://doi.org/10.1617/s11527-014-0509-y.

Kumar, S., Kumar, R., Bandopadhyay, A., Alex, T.C., Ravi Kumar, B., Das, S.K., Mehrotra, S.P., 2008. Mechanical activation of granulated blast furnace slag and its effect on the properties and structure of Portland slag cement. Cem. Concr. Compos. 30, 679–685. https://doi.org/10.1016/j.cemconcomp.2008.05.005.

Li, T., Sui, F., Li, F., Cai, Y., Jin, Z., 2014. Effects of dry grinding on the structure and granularity of calcite and its polymorphic transformation into aragonite. Powder Technol. 254, 338–343. https://doi.org/10.1016/j.powtec.2014.01.043.
Lin, R.S., Wang, X.Y., Zhang, G.Y., 2018. Effects of quartz powder on the microstructure and key properties of cement paste. Sustain. Times 10. https://doi.org/10.3390/su10103369.
Liu, H., Chen, X., Che, J., Liu, N., Zhang, M., 2020. Mechanical performances of concrete produced with desert sand after elevated temperature. Int. J. Concr. Struct. Mater. 14. https://doi.org/10.1186/s40069-020-00402-3.
Liu, M., Liu, E., Hao, J.L., Di Sarno, L., Xia, J., 2023. Hydration and material properties of blended cement with ground desert sand. Constr. Build. Mater. 389, 131624. https://doi.org/10.1016/j.conbuildmat.2023.131624.
Mehdizadeh, H., Ling, T.-C., Cheng, X., Mo, K.H., 2020. Effect of particle size and CO2 treatment of waste cement powder on properties of cement paste. Can. J. Civ. Eng. 531, 522–531. https://doi.org/10.1139/cjce-2019-0574.
Mohamed, A.M.O., El Gamal, M., 2009. Hydro-mechanical behavior of a newly developed sulfur polymer concrete. Cem. Concr. Compos. 31, 186–194. https://doi.org/10.1016/j.cemconcomp.2008.12.006.
Opoczky, L., 1977. Fine grinding and agglomeration of silicates. Powder Technol. 17, 1–7.
Panesar, D.K., Zhang, R., 2020. Performance comparison of cement replacing materials in concrete: limestone fillers and supplementary cementing materials – a review. Constr. Build. Mater. 251, 118866. https://doi.org/10.1016/j.conbuildmat.2020.118866.
Sajedi, F., 2012. Mechanical activation of cement-slag mortars. Constr. Build. Mater. 26, 41–48. https://doi.org/10.1016/j.conbuildmat.2011.05.001.
Sharp, J.H., Gartner, E.M., Macphee, D.E., 2010. Novel cement systems (sustainability). Session 2 of the fred glasser cement science symposium. Adv. Cement Res. 22, 195–202. https://doi.org/10.1680/adcr.2010.22.4.195.
She, A., Ma, K., Liao, G., Yao, W., Zuo, J., 2021. Investigation of hydration and setting process in nanosilica-cement blended pastes: in situ characterization using low field nuclear magnetic resonance. Constr. Build. Mater. 304, 124631. https://doi.org/10.1016/j.conbuildmat.2021.124631.
Souri, A., Kazemi-Kamyab, H., Snellings, R., Naghizadeh, R., Golestani-Fard, F., Scrivener, K., 2015. Pozzolanic activity of mechanochemically and thermally activated kaolins in cement. Cement Concr. Res. 77, 47–59. https://doi.org/10.1016/j.cemconres.2015.04.017.
Suraneni, P., Hajibabaee, A., Ramanathan, S., Wang, Y., Weiss, J., 2019. New insights from reactivity testing of supplementary cementitious materials. Cem. Concr. Compos. 103, 331–338. https://doi.org/10.1016/j.cemconcomp.2019.05.017.
Szabó, R., Kristály, F., Nagy, S., Singla, R., Mucsi, G., Kumar, S., 2023. Reaction, structure and properties of eco-friendly geopolymer cement derived from mechanically activated pumice. Ceram. Int. 49, 6756–6763. https://doi.org/10.1016/j.ceramint.2022.10.204.
Thongsanitgarn, P., Wongkeo, W., Chaipanich, A., Poon, C.S., 2014. Heat of hydration of Portland high-calcium fly ash cement incorporating limestone powder: effect of limestone particle size. Constr. Build. Mater. 66, 410–417. https://doi.org/10.1016/j.conbuildmat.2014.05.060.
Tiwari, S., Kumar, A., Kaur, G., 2022. Visible light-responsive photocatalytic-based sustainable construction material for environmental remediation. Ceram. Int. 49, 11076–11090. https://doi.org/10.1016/j.ceramint.2022.11.304.
Wang, Y., He, X., Su, Y., Yang, J., Strnadel, B., Wang, X., 2019. Efficiency of wet-grinding on the mechano-chemical activation of granulated blast furnace slag (GBFS). Constr. Build. Mater. 199, 185–193. https://doi.org/10.1016/j.conbuildmat.2018.11.245.
Wang, Y., Yuan, Q., Deng, D., Ye, T., Fang, L., 2017. Measuring the pore structure of cement asphalt mortar by nuclear magnetic resonance. Constr. Build. Mater. 137, 450–458. https://doi.org/10.1016/j.conbuildmat.2017.01.109.
Wei, B., Zhang, Y., Bao, S., 2017. Preparation of geopolymers from vanadium tailings by mechanical activation. Constr. Build. Mater. 145, 236–242. https://doi.org/10.1016/j.conbuildmat.2017.03.234.
Wu, P., Lyu, X., Wang, J., Hu, S., 2017. Effect of mechanical grinding on the hydration activity of quartz in the presence of calcium hydroxide. Adv. Cement Res. 29, 269–277. https://doi.org/10.1680/jadcr.16.00159.
Xu, F., Wei, H., Qian, W., Chen, X., Xu, T., He, Y., Wen, G., 2020. Experimental investigation on replacing cement by sintered limestone ash from the steelmaking industry for cement-stabilized soil: engineering performances and micro-scale analysis. Constr. Build. Mater. 235, 117425. https://doi.org/10.1016/j.conbuildmat.2019.117425.
Yan, P., Zhang, Q., 2006. Microstructural characteristics of complex binder paste containing active or inert mineral admixtures, Kuei Suan Jen Hsueh Pao/J. Chinese Ceram. Soc. 34, 1491–1496. https://doi.org/10.14062/j.issn.0454-5648.2006.12.014.
Yao, G., Cui, T., Zhang, J., Wang, J., Lyu, X., 2020b. Effects of mechanical grinding on pozzolanic activity and hydration properties of quartz. Adv. Powder Technol. 31, 4500–4509. https://doi.org/10.1016/j.apt.2020.09.028.
Yao, G., Wang, Q., Wang, Z., Wang, J., Lyu, X., 2020a. Activation of hydration properties of iron ore tailings and their application as supplementary cementitious materials in cement. Powder Technol. 360, 863–871. https://doi.org/10.1016/j.powtec.2019.11.002.
Zhang, A., Yang, W., Ge, Y., Wang, Y., Liu, P., 2020b. Study on the hydration and moisture transport of white cement containing nanomaterials by using low field nuclear magnetic resonance. Constr. Build. Mater. 249, 118788. https://doi.org/10.1016/j.conbuildmat.2020.118788.
Zhang, M., Zhu, X., Shi, J., Liu, B., He, Z., Liang, C., 2022. Utilization of desert sand in the production of sustainable cement-based materials: a critical review. Constr. Build. Mater. 327, 127014. https://doi.org/10.1016/j.conbuildmat.2022.127014.
Zhang, S., Yuan, K., Zhang, J., Guo, J., 2020a. Experimental Study on performance influencing factors and reasonable mixture ratio of desert sand ceramsite lightweight aggregate concrete. Adv. Civ. Eng. 2020. https://doi.org/10.1155/2020/8613932.
Zhao, Y., Gao, J., Liu, C., Chen, X., Xu, Z., 2020. The particle-size effect of waste clay brick powder on its pozzolanic activity and properties of blended cement. J. Clean. Prod. 242, 118521. https://doi.org/10.1016/j.jclepro.2019.118521.